BikeZ-ETH: Mass cycling flow experiments for trajectory data collection

Ying-Chuan Ni

Thomas Ramseier

Shaimaa K. El-Baklish

Kevin Riehl

Anastasios Kouvelas

Michail A. Makridis

STRC Conference Paper 2026

STRC | 26th Swiss Transport Research Conference
Monte Verità / Ascona, May 20-22, 2026

BikeZ-ETH: Mass cycling flow experiments for trajectory data collection

Ying-Chuan Ni
SVT, IVT
ETH Zurich
ying-chuan.ni@ivt.baug.ethz.ch

Thomas Ramseier
SVT, IVT
ETH Zurich
thomas.ramseier@ivt.baug.ethz.ch

Shaimaa K. El-Baklish
SVT, IVT
ETH Zurich
shaimaa.elbaklish@ivt.baug.ethz.ch

Kevin Riehl
SVT, IVT
ETH Zurich
kevin.riehl@ivt.baug.ethz.ch

Anastasios Kouvelas
SVT, IVT
ETH Zurich
kouvelas@ethz.ch

Michail A. Makridis
SVT, IVT
ETH Zurich
mmakridis@ethz.ch

Abstract

Bicycle traffic congestion is already evident in several major cities in the Netherlands and Denmark. However, in contrast to motorized vehicle traffic, the dynamics of bicycle traffic flow–at both microscopic and macroscopic levels–remain insufficiently understood, particularly in congested conditions. To address this gap, we present the BikeZ-ETH dataset, which comprises high-resolution cycling trajectories collected via drone-based observations from both naturalistic and controlled experiments at multiple locations in the city of Zurich, Switzerland. This work first introduces the field experimental design and the data post-processing pipeline. The dataset enables detailed analysis of bicycle flow efficiency and cycling behavior in various road environments. It also captures bi-modal interactions between bicycles and motor vehicles in mixed-traffic conditions. Leveraging empirical insights derived from the trajectory data, future work will develop a SUMO-integrated traffic simulation API tailored for non-lane-based bicycle flow. Both the dataset and simulation tool support a wide range of applications, including bike lane network design, road space allocation, and multi-modal traffic control strategies.

Keywords

Bicycle flow; Cycling behavior; Trajectory data

Preferred citation

Ni, Y.-C., T. Ramseier, S. K. El-Baklish, K. Riehl, A. Kouvelas and M. A. Makridis (2026) BikeZ-ETH: Mass cycling flow experiments for trajectory data collection, paper presented at the *26th Swiss Transport Research Conference (STRC 2026)*, Ascona, May 2026.

Contents

List of Tables

List of Figures

1 Introduction

The promotion of cycling has become a key element of urban mobility strategies worldwide. This trend is largely driven by sustainability objectives, such as the United Nations Sustainable Development Goals, congestion reduction policies, public health, and socio-economical concerns (Pucher and Buehler, 2017; Deenihan and Caulfield, 2014). Public authorities at national and local levels are increasingly investing in cycling infrastructure and reallocating road space to encourage a shift away from private motorized vehicles (Lanvin *et al.*, 2025). Following on the footsteps of the E-Bike City project, which has demonstrated that the massive integration of bicycles into urban transport networks can substantially alleviate congestion, improve the efficiency of road space usage, and offer a flexible substitute for car travel (Ballo *et al.*, 2023; Fulton *et al.*, 2025; Elvarsson *et al.*, 2026; de Freitas *et al.*, 2026), the BikeZ-ETH project aims to study bicycle traffic flow dynamics and quantify the efficiency of cycling as a traffic mode (BikeZ-ETH, 2026).

A major obstacle to the precise understanding of cycling behavior and bicycle traffic flow is the scarcity of high resolution cycling trajectory data. The heterogeneity of movement strategies, complex overtaking maneuvers, and cyclist queue formation can only be understood with realistic and accurate datasets, while aggregated data cannot provide the same level of detail. Unlike research on motorized traffic flow, which has long been using trajectory data to propose new models (Li *et al.*, 2020; Buisson *et al.*, 2025), sufficient high-quality cycling trajectory data for bicycle traffic flow studies are still lacking.

Previous controlled experimental datasets suffer from several limitations, including a small sample size (Liang *et al.*, 2018; Guo *et al.*, 2021), complex interactions between modes without isolation of bicycles, limitation to single-file dynamics (Andresen *et al.*, 2014; Zhao and Zhang, 2017; Jiang *et al.*, 2017), etc. Gavriilidou *et al.* (2019) and Gavriilidou *et al.* (2021) conducted an indoor ring-road cycling experiment and collected video footage from cameras for the analysis microscopic and macroscopic cycling traffic flow characteristics. Wierbos *et al.* (2019) and Wierbos *et al.* (2021) also designed small-scale cycling flow experiment to explore the effect of lane widths on capacity and the impact of queue formations on queue discharge rate. However, the data in these studies were not made openly-available.

There were several studies that collected empirical trajectory data to analyze macroscopic and microscopic bicycle flow properties. Hoogendoorn and Daamen (2016) first attempted to analyze the headway distribution of a bicycle traffic flow. Goñi-Ros *et al.* (2018) and

Yuan *et al.* (2019) then conducted more in-depth investigations of the bicycle flow queue discharge process and the relationship between capacity, jam density, and shockwave speed. Grigoropoulos *et al.* (2022) further evaluated the impact of varying infrastructure designs on the bicycle flow efficiency at signalized intersections. While these studies focused on the macroscopic parameters, Twaddle and Grigoropoulos (2016) analyzed cyclists' speeds and acceleration-deceleration dynamics when crossing a signalized intersection to inform simulation models. For other behaviors, Khan and Raksuntorn (2001) can be considered one the earliest empirical studies on cyclists' free-flow riding behavior. Later on, Mohammed *et al.* (2019) also analyzed cyclists' following and overtaking behaviors by collecting trajectories from videos of bi-directional bicycle paths. Paulsen *et al.* (2019) further explored cyclists' desired speed heterogeneity and its effect on overtaking behavior on bicycle paths. In addition, a large amount of high-quality cycling trajectory data is crucial for the simulation and prediction of cycling movements in mixed-traffic environments (Ni *et al.*, 2023; Li *et al.*, 2023).

Floating bicycle / GPS data from mobile devices, which contain the movement patterns of individuals, have also become a potential source for cycling-related research. They have been utilized mainly in the field of transport planning (Lißner and Huber, 2021). For instance, many studies have investigated cyclists' route choice behavior (Zimmermann *et al.*, 2017; Chen *et al.*, 2018; Ton *et al.*, 2018) and their user-oriented travel behavior (Lißner *et al.*, 2020) with the help of GPS data. Karakaya *et al.* (2020) developed the SimRa platform to acquire GPS data from cyclists. The built-in motion sensors detect near miss incidents in bicycle traffic for safety evaluation. For purposes related to traffic flow modeling, GPS-based trajectories can be useful for the analysis of cyclists' speed and acceleration profile in varying road infrastructure (Ma and Luo, 2016; Berjisian and Bigazzi, 2025; Maurer *et al.*, 2025). Strauss and Miranda-Moreno (2017) and Yuan *et al.* (2025) estimated bicycle traffic delay at signalized intersections using data collected by GPS. However, these types of data are usually sparse, making the applications for in-depth analysis of mass cycling traffic flow phenomena rather difficult.

Unlike the studies mentioned above that used video cameras, Kutsch *et al.* (2025) recently analyzed cyclists' trajectories and several microscopic characteristics on a bicycle lane in the TUMDOT-MUC dataset (Kutsch *et al.*, 2024), which was collected from drones. The advantage of such a novel data collection technique is discussed in Section 2. The same group of researchers then conducted another series of drone-based experiments that focused on the discharging behaviors of bicycle queues at signalized intersections (Schöckel *et al.*, 2026). Still, data in various scenarios and more extensive analysis are required to gain in-depth understanding of bicycle traffic congestion phenomena.

In terms of traffic flow modeling and simulation, research has up to recently been largely focused on motorized traffic. In this context, cycling was often considered a mode of transport of secondary importance, usually modeled similarly to cars by omitting some of its crucial aspects, such as non-lane-based movement characteristics (Kaths, 2023; Ni *et al.*, 2024; Brunner *et al.*, 2024). In addition, the lack of high-quality data hinders the development of a comprehensive cycling flow simulation tool.

To fill these gaps, BikeZ-ETH has generated a large cycling trajectory dataset that encompasses diversified traffic situations in Zurich, Switzerland, by conducting drone-based experiments. This dataset goes beyond bicycle observations by also capturing the interaction of bicycles with other modes.

This paper aims to introduce the experiment campaigns for cycling trajectory data collection in the BikeZ-ETH research project and explain the data format to facilitate their usage by others.

2 Field Experiment Design

In recent years, with the advancement of technologies, unmanned aerial vehicles, or drones, have become a popular tool to monitor vehicle movements due to their flexible, high-angle, and wide-area view. They have first been utilized to collect vehicle trajectories on motorways (Krajewski *et al.*, 2018; Chaudhari *et al.*, 2025). Riehl *et al.* (2025a) and Riehl *et al.* (2025b) conducted controlled experiments and used drones to capture the movements of cars within a closed-loop roundabout. The pNEUMA dataset was known to be the first extensive dataset that contains multi-modal vehicle trajectories in urban road environments collected by flying a swarm of drones (Barmpounakis and Geroliminis, 2020), enabling the investigation of various urban traffic flow phenomena. Later on, the TUMDOT-MUC dataset was also collected in a large-scale aerial drone observation in an urban arterial road (Kutsch *et al.*, 2024, 2025). Ammourah *et al.* (2025) even collected vehicle trajectories by filming them from a helicopter.

Considering the advantages of aerial videography mentioned above, in this project, high-resolution (3840×2160 pixels at a frame rate of 25 fps) trajectories were collected using stationary drones flying approximately 20 meters above ground. Several naturalistic and controlled experiments were conducted on June 16th, June 17th, September 29th, and September 30th in 2025. Naturalistic observations have the benefit of reducing any biases or changes in the behavior of cyclists, which can possibly occur in controlled experiments. These observations were carried out in various locations, including mixed traffic un-/signalized intersections, dedicated bicycle lane segments with different widths, bi-directional bicycle lanes, and roundabouts, during the morning and evening peaks to ensure that sufficient bicycle volumes are captured. Particular care was taken to ensure that the bicycles were clearly visible and not hidden by overhead obstacles. Thus, tracking of their trajectory can be done without any interruption.

On the other hand, the controlled experiments allowed us to generate larger bicycle volumes than one can usually observe in the city of Zurich, while also enabling the design of specific situations of interest, such as merging or crossing of intersecting flows. The experiment was carried out on Baslerstrasse (Locations 12 and 13), an open road, to ensure that realistic interactions with other modes of transport can still be guaranteed. The distinction between human-powered bicycles and electric bicycles was made by using colored jackets visible from the drones, so that both types of bicycles can be distinguished. The number of participants in the controlled experiment amounted to 58, which was sufficient to create the desired mass cycling traffic flow situations and, in particular, to observe enough overtaking maneuvers and long waiting queues.

The observed locations in Zurich are summarized in Table 1 and Figure 1. Locations 1, 12 and 13 correspond to the controlled experiment locations. The collection and extraction of trajectories at Location 1 was detailed in Riehl *et al.* (2026). Other locations all contain 80 - 160 minutes of video recordings.

Table 1: List of experiment locations in the city of Zurich

No.	**Location**	**No.**	**Location**
1	Albert-Einstein-Str. roundabout	2	Gessnerbrücke - Kasernenstr.
3	Gessnerbrücke - Gessnerallee	4	Zollstr. - Langstr.
5	Zollstr. - Klingenstr.	6	Quaibrücke
7	Bullingerplatz	8	Duttweilerbrücke
9	Bullingerstr. - Herdenstr.	10	Birmensdorferstr. - Gutstr.
11	Birmensdorferstr. - Schweighofstr.	12	Baslerstr. - Freihofstr.
13	Baslerstr. - Flurstr.		

Figure 2 shows several screenshots from the drone video recordings. The red-highlighted

Figure 1: Locations of the drone-based BikeZ-ETH experiment campaign in the city of Zurich, Switzerland

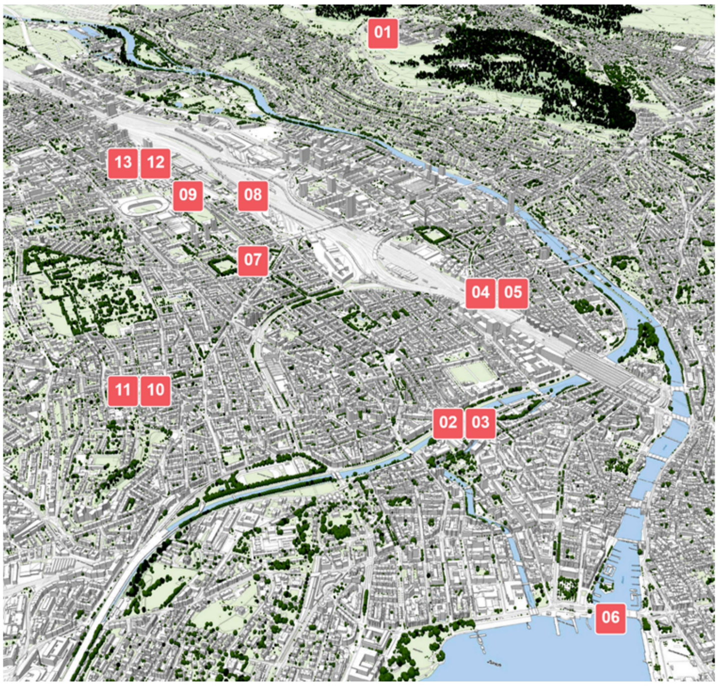

Figure 2: Screenshot from the video recordings at Locations 2 (upper-left), 6 (upper-right), 7 (lower-left), and 13 (lower-right) of the drone-based experiment campaign

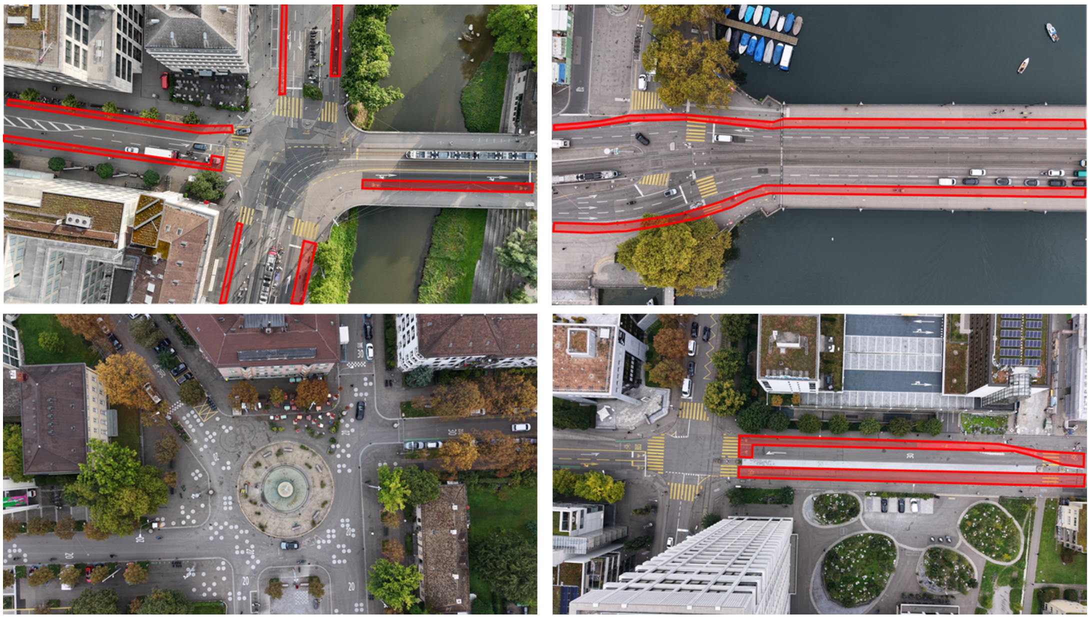

areas are dedicated bicycle lanes. Location 2 captures the acceleration-deceleration dynamics and queue formations of bicycles around an intersection. Varying lane widths from 1.0 to 3.5 m can be found. Location 6 contains the free-flow, following, and overtaking behaviors on long stretches of dedicated bicycle lanes. Location 7 is a low-speed mixed-traffic roundabout. And one of the controlled experiments is conducted on the wide bicycle lanes at Location 13.

Figure 3 shows the identification of bicycles (red shapes) on a 2.5-m-wide dedicated lane while the cyclists queued up before the stop line at an intersection in Location 13. Through analyzing the trajectories at these moments, one can understand cyclists' queue formation and the jam density of bicycle flow under different lane widths.

Figure 3: Bicycles identification while queuing taken from location 13

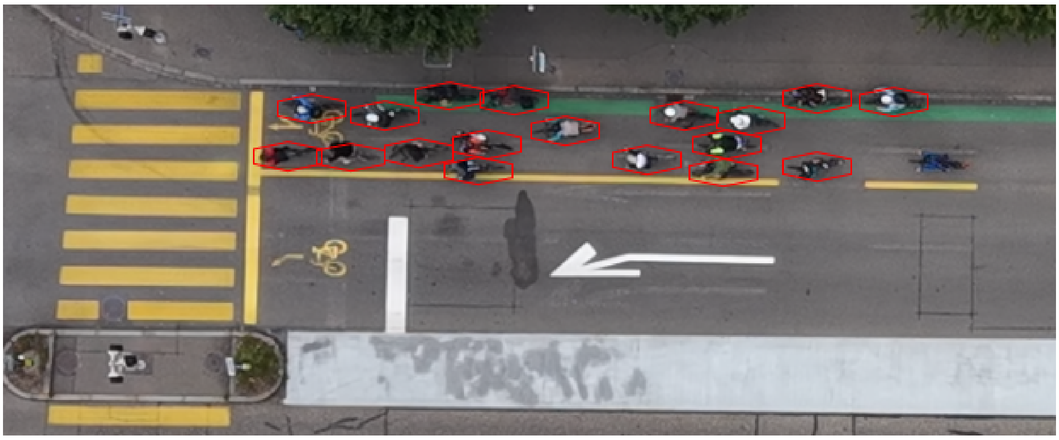

The collected videos, in the form of stationary top-down videos, were subsequently processed and extracted by MobiLysis Sàrl (MobiLysis, 2026) using their in-house computer vision tool to identify the absolute positions of the cyclists. Figure 4 shows the trajectories observed in a 20-minute period at Location 2.

3 Data Processing

Vehicle and bicycle movements in urban road networks are complex due to multi-modality, varying infrastructure, and numerous possible travel directions. To enhance the applicability and reproducibility of the collected trajectories in research (Buisson *et al.*, 2025), the raw trajectories are first filtered and completed before being transformed into lane-based coordinates. Raw tracking data inevitably contain noise and, in the case of bicycles,

Figure 4: Collected bicycle trajectories in a 20-minute period at Locations 2 (upper-left), 4 (upper-right), 9 (lower-left), and 10 (lower-right)

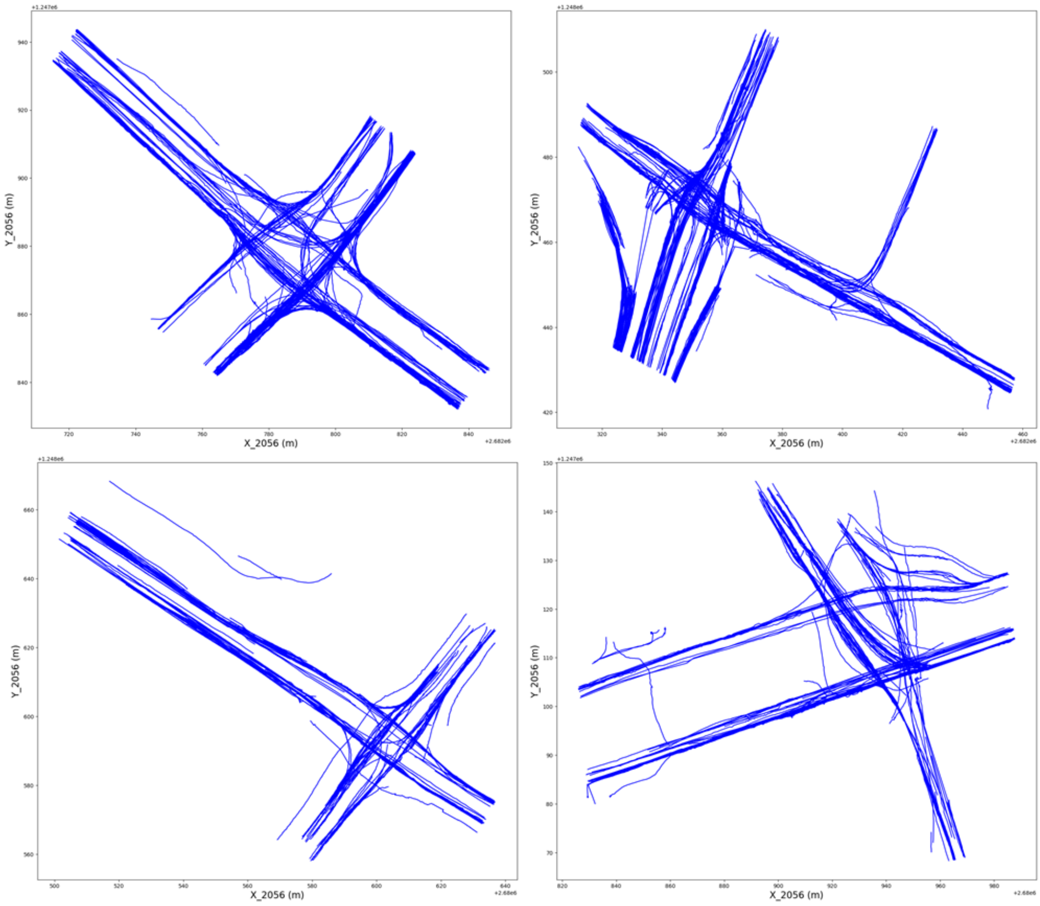

gaps caused by camera occlusion. Trajectory gaps arise when a cyclist passes through an occluded region of the camera field of view. As shown in Figure 5, gaps affect between 1–3% of bicycles per session, while motorized vehicles exhibit virtually no occlusion gaps. Gap durations (Figure 5, left subplot) have a median of 1.76 s and a mean of 2.38 s (std. 1.65 s), with occasional extremes exceeding 9 s. At 25 fps, a median gap corresponds to over 40 missing frames — far too long to bridge reliably by extended Kalman filter (EKF) predict-only, which accumulates unbounded position uncertainty in the absence of observations. This motivates a dedicated geometric inference step prior to filtering.

For each detected gap, we construct a path that satisfies $\mathcal{G}_2$ continuity — that is, position, heading, and curvature are matched simultaneously at both gap boundaries. This is stronger than the $\mathcal{C}_1$ continuity of linear or spline interpolation, which only guarantees positional smoothness, and is physically motivated by the fact that a cyclist cannot

Figure 5: Gap length distributions per location and date

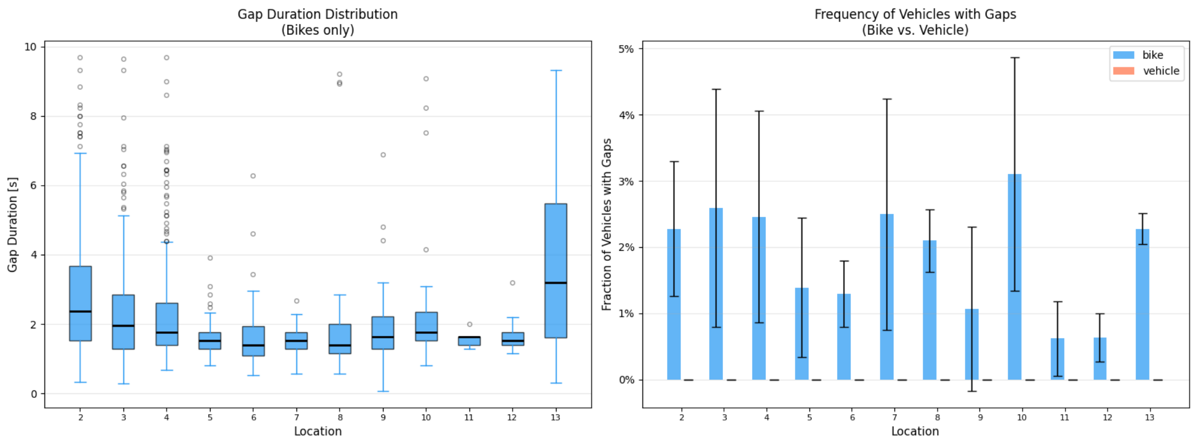

instantaneously change their turning radius. A clothoid (Euler spiral) is the natural curve class for this purpose, as its curvature varies linearly with arc-length, closely approximating the steering behaviour of a bicycle (Levien, 2008; Silva and Grassi, 2018). Boundary headings are estimated from finite differences of neighbouring observed positions, and boundary curvatures are derived from the circumscribed circle of a Gaussian-smoothed window of observations. A speed profile $v(t)$ is then optimized along the fixed clothoid geometry, parameterized as a Bernstein polynomial to guarantee $v(t) \geq 0$ by construction. The angular velocity is recovered geometrically as $\omega(t) = \kappa(s(t)) \cdot v(t)$, decoupling the geometric and dynamic sub-problems. The full procedure is summarized in Algorithm 1.

The inferred states are inserted as pseudo-observations into the trajectory before filtering. A unicycle kinematic model is adopted, with state vector $\mathbf{x} = [x, y, v, \theta]^\top$ and $\mathbf{u} = [a, \omega]^\top$. An Extended Kalman Filter (EKF) (Kalman, 1960) performs forward predict-correct passes over the full sequence; gap pseudo-observations are down-weighted by inflating their measurement noise covariance to $\mathbf{R}_{\text{gap}} = 4\mathbf{R}$, reflecting the additional uncertainty of the clothoid inference relative to direct observations. A Rauch-Tung-Striebel (RTS) smoother (Rauch *et al.*, 1965) then performs a backward pass, retroactively tightening all state estimates using future information.

Figure 6 illustrates the filtering pipeline for two representative cases. In both examples, the left subplot shows the XY trajectory with raw observations, the EKF+RTS filtered path, and the clothoid-inferred gap segment highlighted in orange; whereas the right subplot shows the corresponding speed, acceleration, and angular velocity time series with the gap region shaded. Vehicle 498 (2025-06-17, location 4, AM3) presents a long gap of

Algorithm 1 Gap Inference Algorithm

Require: Trajectory $\mathcal{T} = \{(\mathbf{x}_i, t_i)\}_{i=1}^N$, gap threshold τ (default 1 s), noise ratio α (default 4), Bernstein degree K (default 5)

Ensure: Pseudo-observations filling all long gaps; gap registry $\mathcal{G}$

for each contiguous gap $[t_s, t_e]$ in $\mathcal{T}$ **do**
  if $(t_e - t_s) \leq \tau$ **then**
    skip ▷ Short gap: handled by EKF predict-only
  end if
  Stage 1 — Geometry
  Estimate boundary headings θ_s, θ_e via $\arctan2(\Delta y, \Delta x)$ on observed neighbours
  Estimate boundary curvatures κ_s, κ_e via circumscribed circle on Gaussian-smoothed window
  Solve G2 clothoid: $\mathcal{C} \leftarrow \textsc{SolveG2}(\mathbf{p}_s, \theta_s, \kappa_s,\ \mathbf{p}_e, \theta_e, \kappa_e)$
  Compute total arc-length $S = \int_{\mathcal{C}} ds$
  Stage 2 — Speed Profile
  Parameterize $v(t)$ as degree-K Bernstein polynomial with control points $\mathbf{c} \geq 0$
  Pin boundary conditions: $v(t_s) = v_s,\ v(t_e) = v_e$
  Recover angular velocity geometrically: $\omega(t) = \kappa(s(t)) \cdot v(t)$
  Solve:

$$\mathbf{c}^* = \arg\min_{\mathbf{c}\geq 0} \underbrace{\|\mathbf{p}(t_e) - \mathbf{p}_e\|^2}_{\text{endpoint}} + \lambda_1\|\Delta a\|^2 + \lambda_2\|\Delta\omega\|^2 + \lambda_3\mathcal{L}_{\text{bnd}}$$

  Normalize: $v^*(t) \leftarrow v^*(t) \cdot S \big/ \int_{t_s}^{t_e} v^*(t)\, dt$ ▷ Guarantees rollout reaches $\mathbf{p}_e$
  Pseudo-observation Fill
  Roll out $(x(t), y(t), \theta(t))$ along $\mathcal{C}$ using $s(t) = \int_0^t v^*(\tau)\, d\tau$
  Insert rolled-out states as pseudo-observations with $\mathbf{R}_{\text{gap}} = \alpha \cdot \mathbf{R}$
  Register gap in $\mathcal{G}$
end for

6.44 s through a sharp turn — the most demanding scenario for the inference algorithm. The speed profile drops to near-zero before recovering, consistent with a cyclist slowing to navigate the bend, and no discontinuity in heading or speed is observed at either boundary. Vehicle 196 (2025-06-17, location 2, PM1) illustrates a shorter gap of 2.24 s through a curved segment, where the clothoid smoothly connects the observed trajectory with continuous acceleration and angular velocity profiles at both boundaries.

Each filtered trajectory is subsequently projected onto a curvilinear lane coordinate system defined by the road centerlines. Centerlines are derived from OpenStreetMap (OpenStreetMap, 2025; Boeing, 2017) and refined against swisstopo orthoimagery (Federal Office of Topography swisstopo, 2025) to ensure geometric accuracy at the intersection level. Turn connections between approach and departure segments are modelled as $\mathcal{G}_2$-continuous

Figure 6: Gap inference and EKF+RTS filtering for two representative bicycles

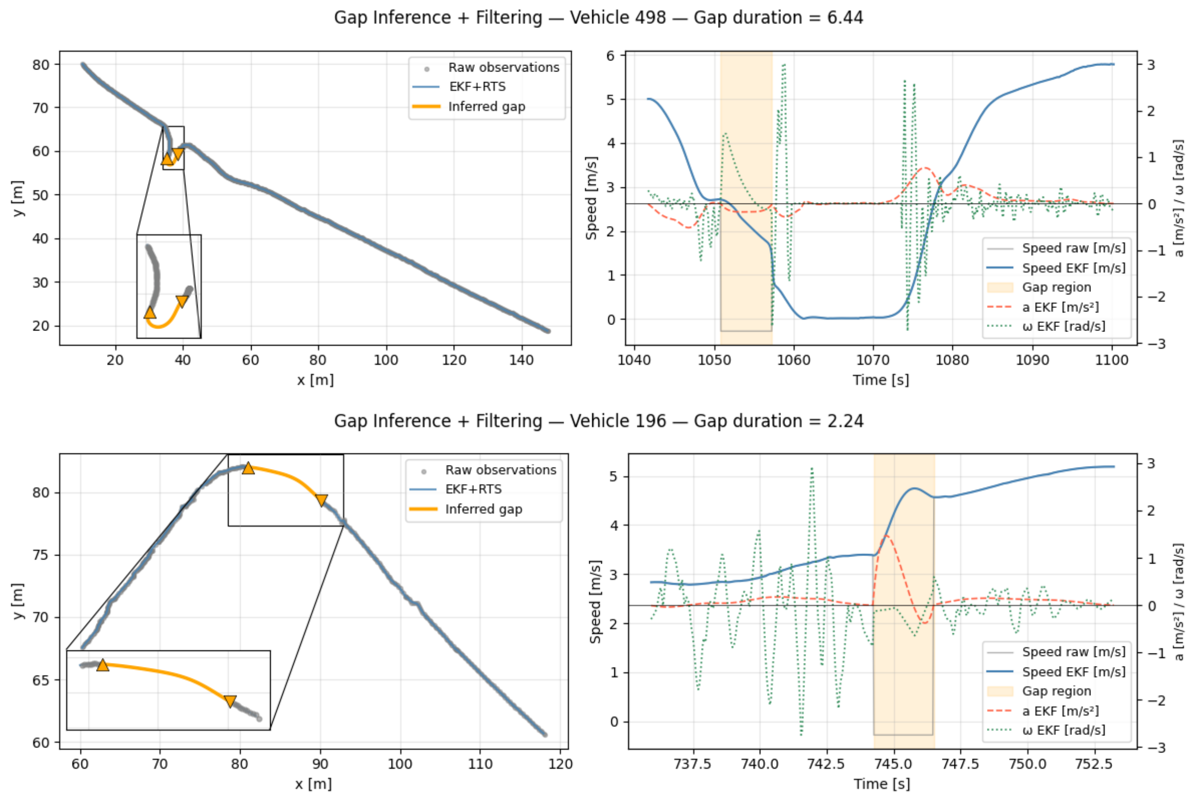

clothoids (Casal *et al.*, 2017), consistent with the gap inference geometry described above. Each filtered position $\mathbf{p} = (x, y)^\top$ is projected onto the nearest centerline B-spline $\mathbf{c}(t)$ by solving:

$$t^* = \arg\min_{t\in[0,1]} \|\mathbf{p} - \mathbf{c}(t)\|^2 \tag{1}$$

via warm-started Newton refinement. The longitudinal coordinate is the arc-length $s = \int_0^{t^*} \|\mathbf{c}'(\tau)\| d\tau$, and the signed lateral offset is:

$$d = (\mathbf{p} - \mathbf{c}(t^*)) \cdot \hat{\mathbf{n}}(t^*) \tag{2}$$

where $\hat{\mathbf{t}} = \frac{\mathbf{c}'(t^*)}{\|\mathbf{c}'(t^*)\|}$ is the unit tangent and $\hat{\mathbf{n}} = [-\hat{t}_y, \hat{t}_x]^\top$ is the unit normal, with $d > 0$ to the left of the direction of travel. The longitudinal and lateral velocity and acceleration components are then obtained by projection onto the local Frenet frame:

$$\dot{s} = \mathbf{v} \cdot \hat{\mathbf{t}}, \quad \dot{d} = \mathbf{v} \cdot \hat{\mathbf{n}}, \quad \ddot{s} = \mathbf{a} \cdot \hat{\mathbf{t}}, \quad \ddot{d} = \mathbf{a} \cdot \hat{\mathbf{n}} \tag{3}$$

where $\mathbf{v} = v(\cos\theta, \sin\theta)^\top$ and $\mathbf{a} = a(\cos\theta, \sin\theta)^\top$ are constructed from the EKF+RTS estimates of speed v, heading θ, and acceleration a. Segment matching assigns each trajectory to an approach, turn, or departure role, enabling movement-level analysis across the intersection. Figure 7 illustrates the transformation for a representative bicycle trajectory.

Figure 7: Lane coordinate transformation for a representative bicycle (Location 4)

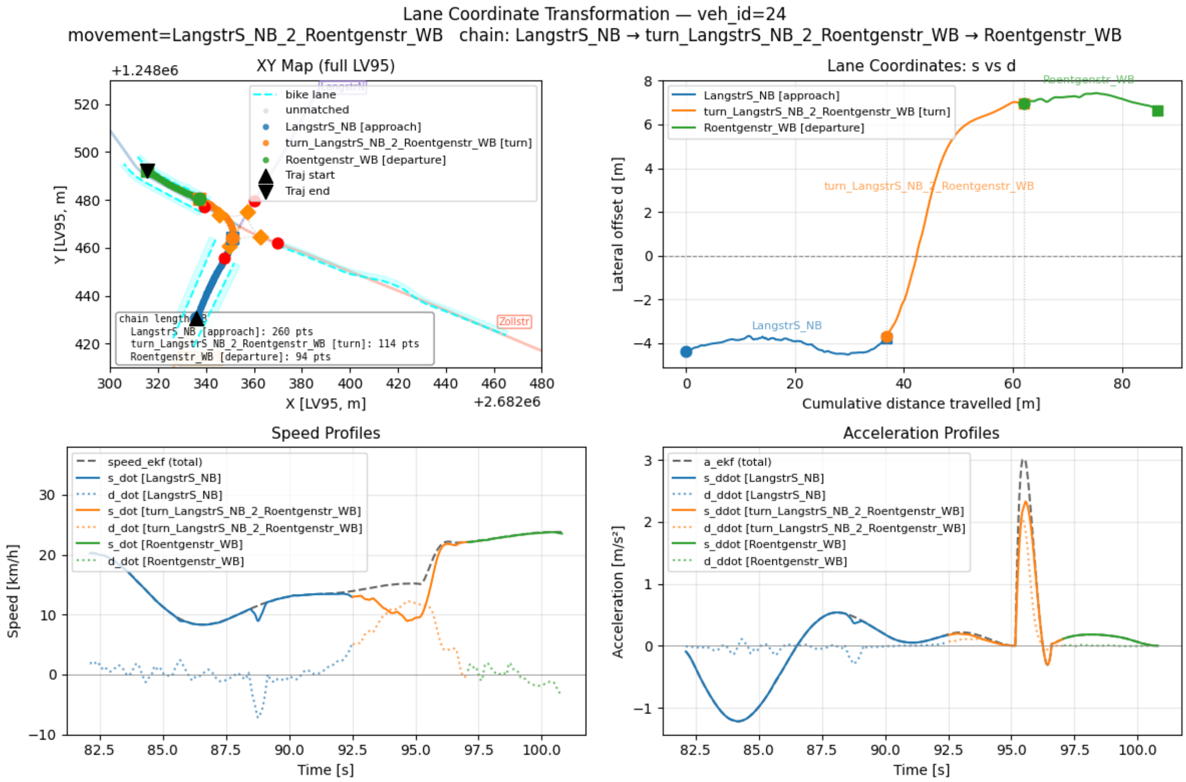

It is worth mentioning that car trajectories are also processed from the videos and filtered using the same method as the bicycle trajectories. The full set of processed attributes is summarised in Table 2. For each trajectory, the table lists the EKF+RTS kinematic estimates, the lane coordinate outputs $(s, d, \dot{s}, \dot{d}, \ddot{s}, \ddot{d})$, and the diagnostic flags enabling downstream lane-level and movement-level analysis.

Due to privacy concerns, we decided not to publish the recorded videos although they were recorded from a sufficiently high distance above ground. Alternatively, the filtered trajectories are replicated as time-stamped animations, providing a visual equivalent of the raw footage without exposing identifiable information. The data and replicated animations will be made available and can be accessed via this website: `https://www.bikez.ethz.ch/`.

Table 2: Processed trajectory data attributes.

Attribute	**Unit**	**Description**
Identifiers and timestamps		
`veh_id`	-	Unique vehicle identifier
`veh_type`	-	Vehicle type (bike, car, truck, bus)
t	s	Elapsed time from recording start
`datetime`	-	Global timestamp (Swiss local time)
Filtered kinematic state		
x_{ekf}, y_{ekf}	m	EKF+RTS smoothed position in local EPSG:2056 coordinates
v_{ekf}	km/h	EKF+RTS smoothed speed
a_{ekf}	m/s^2	EKF+RTS smoothed acceleration
θ_{ekf}	rad	EKF+RTS estimated heading angle
ω_{ekf}	rad/s	EKF+RTS estimated angular velocity
Lane coordinates		
s	m	Arc-length along the segment centerline in the direction of travel, reset to 0 at segment entry
d	m	Signed lateral offset from centerline; positive = left of travel direction
$\dot{s}$	km/h	Longitudinal speed component along centerline tangent
$\dot{d}$	km/h	Lateral speed component along centerline normal
$\ddot{s}$	m/s^2	Longitudinal acceleration along centerline tangent
$\ddot{d}$	m/s^2	Lateral acceleration along centerline normal
Flags and diagnostics		
`missing`	-	Boolean; `True` if data entry was missing initially (i.e. a gap that was hence inferred)
`movement_key`	-	Named movement assigned to the trajectory (e.g. approach-turn-departure)
`segment_id`	-	Key of the matched segment within the movement
`in_bike_lane`	-	Boolean; `True` if lateral position falls within dedicated bike lane boundary (± 0.2 m tolerance)
`d_to_bike_boundary`	m	Signed lateral distance to the near edge of the bike lane; negative = inside, positive = outside

4 Conclusions and Ongoing Work

The BikeZ-ETH project will contribute to improving the current understanding of the dynamics of bicycle traffic flow. To do so, an open source bicycle trajectory dataset collected via drone-based controlled and naturalistic experiments in various urban road environments will be published.

The trajectories will first be used for the analysis of bicycle fundamental diagrams (BFDs) with complete traffic regimes under different bicycle lane widths. A BFD reflects several macroscopic bicycle flow parameters and provides a way to quantify the efficiency of bicycle flow in comparison to car traffic. In addition, the data enable us to investigate microscopic cycling behavior in different action states, such as free-flow, following, overtaking in uninterrupted flow situations, and discharging, stopping, or queueing in interrupted flow situations with traffic lights.

Other relevant works within the project include an open source microscopic bicycle simulation API implemented in SUMO, an open-source software package (Lopez *et al.*, 2018). It is developed to improve the mass cycling flow simulation by capturing the unique characteristics of this traffic mode. Furthermore, the analyzed macroscopic bicycle flow properties will be used to develop advanced car-bicycle road space allocation strategies that take traffic efficiency into account.

Furthermore, the collected trajectories can also be used to assess the traffic safety performance of various infrastructure designs by analyzing the conflict indicators, such as time-to-collision and post-encroachment time, for bicycle-bicycle and car-bicycle interactions (van der Horst *et al.*, 2014; Madsen and Lahrmann, 2017).

The contributions of BikeZ-ETH will facilitate accurate planning and management of future road networks with a large cycling modal share, which is a crucial requirement to improve the sustainability of cities throughout the world. The quantitative findings and the developed simulation tool can assist traffic engineers and urban planners in their decision-making. The emphasis on openly accessible data and models will also further improve the reproducibility of research in the field of multi-modal urban transport systems by providing useful benchmarks for researchers.

Acknowledgments

This project is funded by Innosuisse under the grant “BikeZ: Model Suite for Mass Cycling as a Service Simulation” Innovation project (grant agreement: 123.077 IP-SBM).

5 References

Ammourah, R., P. Beigi, B. Fan, S. H. Hamdar, J. Hourdos, C.-C. Hsiao, R. James, M. Khajeh-Hosseini, H. S. Mahmassani, D. Monzer, T. Radvand, A. Talebpour, M. Yousefi and Y. Zhang (2025) Introduction to the Third Generation Simulation Dataset: Data Collection and Trajectory Extraction, *Transportation Research Record: Journal of the Transportation Research Board*, **2679** (1) 1768–1784, 1 2025, ISSN 0361-1981.

Andresen, E., M. Chraibi, A. Seyfried and F. Huber (2014) Basic Driving Dynamics of Cyclists, in *Simulation of Urban Mobility: First International Conference*, 18–32.

Ballo, L., L. M. de Freitas, A. Meister and K. W. Axhausen (2023) The E-Bike City as a radical shift toward zero-emission transport: Sustainable? Equitable? Desirable?, *Journal of Transport Geography*, **111**, 103663, 7 2023, ISSN 09666923.

Barmpounakis, E. and N. Geroliminis (2020) On the new era of urban traffic monitoring with massive drone data: The pNEUMA large-scale field experiment, *Transportation Research Part C: Emerging Technologies*, **111**, 50–71, 2 2020, ISSN 0968090X.

Berjisian, E. and A. Bigazzi (2025) Identification and investigation of cruising speeds from cycling GPS data, *Transportation*, 3 2025, ISSN 0049-4488.

BikeZ-ETH (2026) BikeZ-ETH: An openly available bicycle trajectory dataset & a mass cycling traffic flow simulation tool, `https://bikez.ethz.ch/`.

Boeing, G. (2017) OSMnx: New methods for acquiring, constructing, analyzing, and visualizing complex street networks, *Computers, Environment and Urban Systems*, **65**, 126–139, 9 2017, ISSN 01989715.

Brunner, J. S., Y.-C. Ni, A. Kouvelas and M. A. Makridis (2024) Microscopic simulation of bicycle traffic flow incorporating cyclists' heterogeneous dynamics and non-lane-based movement strategies, *Simulation Modelling Practice and Theory*, **135**, 102986, 9 2024, ISSN 1569190X.

Buisson, C., R. Slama, Z. Zheng, M. A. Arman, B. Coifman, B. Ciuffo, D. Gloudemans, S. Hamdar, X. Hu, J. Ji, R. Jiang, A. Maji, M. Makridis, H. Mahmassani, M. Montanino, V. Punzo, C. Tampere, A. Talebpour, J. Tian, D. Work and S.-T. Zheng (2025) Trajectory data collecting and sharing:Where are we? Where shall we go?, 10 2025.

Casal, G., D. Santamarina and M. E. Vázquez-Méndez (2017) Optimization of horizontal alignment geometry in road design and reconstruction, *Transportation Research Part C: Emerging Technologies*, **74**, 261–274, 1 2017, ISSN 0968090X.

Chaudhari, A. A., M. Treiber and O. Okhrin (2025) MiTra: A Drone-Based Trajectory Data for an All-Traffic-State Inclusive Freeway with Ramps, *Scientific Data*, **12** (1) 1174, 7 2025, ISSN 2052-4463.

Chen, P., Q. Shen and S. Childress (2018) A GPS data-based analysis of built environment influences on bicyclist route preferences, *International Journal of Sustainable Transportation*, **12** (3) 218–231, 3 2018, ISSN 1556-8318.

de Freitas, L. M., M. Miotti, D. Zani and K. W. Axhausen (2026) Rethinking cost–benefit analysis for transformative cycling policies: Integrating behavioral change and the logsum method, *Transport Policy*, **182**, 104112, 7 2026, ISSN 0967070X.

Deenihan, G. and B. Caulfield (2014) Estimating the health economic benefits of cycling, *Journal of Transport & Health*, **1** (2) 141–149, 6 2014, ISSN 22141405.

Elvarsson, A., D. Zani and B. T. Adey (2026) Fast-lane for planning cycling infrastructure: On the effectiveness and efficiency of cycling infrastructure planning processes, *Journal of Cycling and Micromobility Research*, **7**, 100103, 3 2026, ISSN 29501059.

Federal Office of Topography swisstopo (2025) Orthophotos — Aerial Images of Switzerland, `https://www.swisstopo.admin.ch`.

Fulton, E. J., Y.-C. Ni and A. Kouvelas (2025) Impact of radical bike lane allocation on bi-modal urban road network traffic performance: A simulation case study, *Case Studies on Transport Policy*, **22**, 101583, 12 2025, ISSN 2213624X.

Gavriilidou, A., W. Daamen, Y. Yuan, N. van Nes and S. Hoogendoorn (2021) Empirical findings on infrastructure efficiency at a bicycle T-junction, *Physica A: Statistical Mechanics and its Applications*, **567**, 125675, 4 2021, ISSN 03784371.

Gavriilidou, A., M. J. Wierbos, W. Daamen, Y. Yuan, V. L. Knoop and S. P. Hoogendoorn (2019) Large-Scale Bicycle Flow Experiment: Setup and Implementation, *Transportation Research Record: Journal of the Transportation Research Board*, **2673** (5) 709–719, 5 2019, ISSN 0361-1981.

Goñi-Ros, B., Y. Yuan, W. Daamen and S. P. Hoogendoorn (2018) Empirical Analysis of the Macroscopic Characteristics of Bicycle Flow during the Queue Discharge Process at a Signalized Intersection, *Transportation Research Record: Journal of the Transportation Research Board*, **2672** (36) 51–62, 12 2018, ISSN 0361-1981.

Grigoropoulos, G., A. Leonhardt, H. Kaths, M. Junghans, M. M. Baier and F. Busch (2022) Traffic flow at signalized intersections with large volumes of bicycle traffic, *Transportation Research Part A: Policy and Practice*, **155**, 464–483, 1 2022, ISSN 09658564.

Guo, N., R. Jiang, S. Wong, Q.-Y. Hao, S.-Q. Xue and M.-B. Hu (2021) Bicycle flow dynamics on wide roads: Experiments and simulation, *Transportation Research Part C: Emerging Technologies*, **125**, 103012, 4 2021, ISSN 0968090X.

Hoogendoorn, S. and W. Daamen (2016) Bicycle Headway Modeling and Its Applications, *Transportation Research Record: Journal of the Transportation Research Board*, **2587** (1) 34–40, 1 2016, ISSN 0361-1981.

Jiang, R., M.-B. Hu, Q.-S. Wu and W.-G. Song (2017) Traffic Dynamics of Bicycle Flow: Experiment and Modeling, *Transportation Science*, **51** (3) 998–1008, 8 2017, ISSN 0041-1655.

Kalman, R. E. (1960) A New Approach to Linear Filtering and Prediction Problems, *Journal of Basic Engineering*, **82** (1) 35–45, 3 1960, ISSN 0021-9223.

Karakaya, A.-S., J. Hasenburg and D. Bermbach (2020) SimRa: Using crowdsourcing to identify near miss hotspots in bicycle traffic, *Pervasive and Mobile Computing*, **67**, 101197, 9 2020, ISSN 15741192.

Kaths, H. (2023) A movement and interaction model for cyclists and other non-lane-based road users, *Frontiers in Future Transportation*, **4**, 10 2023, ISSN 2673-5210.

Khan, S. I. and W. Raksuntorn (2001) Characteristics of Passing and Meeting Maneuvers on Exclusive Bicycle Paths, *Transportation Research Record: Journal of the Transportation Research Board*, **1776** (1) 220–228, 1 2001, ISSN 0361-1981.

Krajewski, R., J. Bock, L. Kloeker and L. Eckstein (2018) The highD Dataset: A Drone Dataset of Naturalistic Vehicle Trajectories on German Highways for Validation of Highly Automated Driving Systems, paper presented at the *2018 21st International*

Conference on Intelligent Transportation Systems (ITSC), 2118–2125, 11 2018, ISBN 978-1-7281-0321-1.

Kutsch, A., L. Kessler and K. Bogenberger (2025) Analyzing Bicycle Riding Characteristics Based on Naturalistic Urban Drone Observations: Free Riding, Following Behavior, and Overtaking Maneuvers, *Transportation Research Record: Journal of the Transportation Research Board*, **2679** (9) 900–914, 9 2025, ISSN 0361-1981.

Kutsch, A., M. Margreiter and K. Bogenberger (2024) TUMDOT–MUC: Data Collection and Processing of Multimodal Trajectories Collected by Aerial Drones, *Data Science for Transportation*, **6** (2) 15, 8 2024, ISSN 2948-135X.

Lanvin, A., J. Charléty, G. Ferreol, A. Homann, E. Massey, A. Vermeulen and A. Chasse (2025) How to create a sustainable growth in bicycle traffic? The case of Paris, *Journal of Cycling and Micromobility Research*, **5**, 100081, 9 2025, ISSN 29501059.

Levien, R. (2008) The Euler spiral: a mathematical history, *Technical Report*.

Li, J., Y. Ni and J. Sun (2023) A two-layer integrated model for cyclist trajectory prediction considering multiple interactions with the environment, *Transportation Research Part C: Emerging Technologies*, **155**, 104304, 10 2023, ISSN 0968090X.

Li, L., R. Jiang, Z. He, X. M. Chen and X. Zhou (2020) Trajectory data-based traffic flow studies: A revisit, *Transportation Research Part C: Emerging Technologies*, **114**, 225–240, 5 2020, ISSN 0968090X.

Liang, X., M. Xie and X. Jia (2018) New Microscopic Dynamic Model for Bicyclists' Riding Strategies, *Journal of Transportation Engineering, Part A: Systems*, **144** (8), 8 2018, ISSN 2473-2907.

Lißner, S. and S. Huber (2021) Facing the needs for clean bicycle data – a bicycle-specific approach of GPS data processing, *European Transport Research Review*, **13** (1) 8, 12 2021, ISSN 1867-0717.

Lißner, S., S. Huber, P. Lindemann, J. Anke and A. Francke (2020) GPS-data in bicycle planning: "Which cyclist leaves what kind of traces?" Results of a representative user study in Germany, *Transportation Research Interdisciplinary Perspectives*, **7**, 100192, 9 2020, ISSN 25901982.

Lopez, P. A., E. Wiessner, M. Behrisch, L. Bieker-Walz, J. Erdmann, Y.-P. Flotterod,

R. Hilbrich, L. Lucken, J. Rummel and P. Wagner (2018) Microscopic Traffic Simulation using SUMO, paper presented at the *2018 21st International Conference on Intelligent Transportation Systems (ITSC)*, 2575–2582, 11 2018, ISBN 978-1-7281-0321-1.

Ma, X. and D. Luo (2016) Modeling cyclist acceleration process for bicycle traffic simulation using naturalistic data, *Transportation Research Part F: Traffic Psychology and Behaviour*, **40**, 130–144, 7 2016, ISSN 13698478.

Madsen, T. K. O. and H. Lahrmann (2017) Comparison of five bicycle facility designs in signalized intersections using traffic conflict studies, *Transportation Research Part F: Traffic Psychology and Behaviour*, **46**, 438–450, 4 2017, ISSN 13698478.

Maurer, L. F., A. Meister and K. W. Axhausen (2025) Cycling speed profiles from GPS data: Insights for conventional and electrified bicycles in Switzerland, *Journal of Cycling and Micromobility Research*, **5**, 100077, 9 2025, ISSN 29501059.

MobiLysis (2026) Mobility Solutions as All-In-One Service - MobiLysis, `https://mobilysis.ch/`.

Mohammed, H., A. Y. Bigazzi and T. Sayed (2019) Characterization of bicycle following and overtaking maneuvers on cycling paths, *Transportation Research Part C: Emerging Technologies*, **98**, 139–151, 1 2019, ISSN 0968090X.

Ni, Y., Y. Li, Y. Yuan and J. Sun (2023) An operational simulation framework for modelling the multi-interaction of two-wheelers on mixed-traffic road segments, *Physica A: Statistical Mechanics and its Applications*, **611**, 128441, 2 2023, ISSN 03784371.

Ni, Y.-C., M. A. Makridis and A. Kouvelas (2024) Bicycle as a traffic mode: From microscopic cycling behavior to macroscopic bicycle flow, *Journal of Cycling and Micromobility Research*, **2**, 100022, 12 2024, ISSN 29501059.

OpenStreetMap (2025) Planet OSM, `https://planet.osm.org`.

Paulsen, M., T. K. Rasmussen and O. A. Nielsen (2019) Fast or forced to follow: A speed heterogeneous approach to congested multi-lane bicycle traffic simulation, *Transportation Research Part B: Methodological*, **127**, 72–98, 9 2019, ISSN 01912615.

Pucher, J. and R. Buehler (2017) Cycling towards a more sustainable transport future, *Transport Reviews*, **37** (6) 689–694, 11 2017, ISSN 0144-1647.

Rauch, H. E., F. Tung and C. T. Striebel (1965) Maximum likelihood estimates of linear dynamic systems, *AIAA Journal*, **3** (8) 1445–1450, 8 1965, ISSN 0001-1452.

Riehl, K., S. K. El-Baklish, A. Kouvelas and M. A. Makridis (2025a) Aerial video & trajectory dataset of vehicles on circular road, *Data in Brief*, **61**, 111858, 8 2025, ISSN 23523409.

Riehl, K., S. K. El-Baklish, A. Kouvelas and M. A. Makridis (2025b) Consistent vehicle trajectory extraction from aerial recordings using oriented object detection, *Scientific Reports*, **15** (1) 27522, 7 2025, ISSN 2045-2322.

Riehl, K., S. K. El-Baklish, Y.-C. Ni, A. Kouvelas and M. A. Makridis (2026) BikeZ-ETH – A Mass-Cycling Trajectory Dataset from a Controlled Experiment, *Scientific Data*, 4 2026, ISSN 2052-4463.

Schöckel, A., L. Kessler and K. Bogenberger (2026) Bicycle queues at signalized intersections — A drone-based empirical analysis of headways, saturation flows, and time losses, *Journal of Cycling and Micromobility Research*, **8**, 100117, 6 2026, ISSN 29501059.

Silva, J. A. R. and V. Grassi (2018) Clothoid-Based Global Path Planning for Autonomous Vehicles in Urban Scenarios, paper presented at the *2018 IEEE International Conference on Robotics and Automation (ICRA)*, 4312–4318, 5 2018, ISBN 978-1-5386-3081-5.

Strauss, J. and L. F. Miranda-Moreno (2017) Speed, travel time and delay for intersections and road segments in the Montreal network using cyclist Smartphone GPS data, *Transportation Research Part D: Transport and Environment*, **57**, 155–171, 12 2017, ISSN 13619209.

Ton, D., D. Duives, O. Cats and S. Hoogendoorn (2018) Evaluating a data-driven approach for choice set identification using GPS bicycle route choice data from Amsterdam, *Travel Behaviour and Society*, **13**, 105–117, 10 2018, ISSN 2214367X.

Twaddle, H. and G. Grigoropoulos (2016) Modeling the Speed, Acceleration, and Deceleration of Bicyclists for Microscopic Traffic Simulation, *Transportation Research Record: Journal of the Transportation Research Board*, **2587** (1) 8–16, 1 2016, ISSN 0361-1981.

van der Horst, A. R. A., M. de Goede, S. de Hair-Buijssen and R. Methorst (2014) Traffic conflicts on bicycle paths: A systematic observation of behaviour from video, *Accident Analysis & Prevention*, **62**, 358–368, 1 2014, ISSN 00014575.

Wierbos, M., V. Knoop, R. Bertini and S. Hoogendoorn (2021) Influencing the queue configuration to increase bicycle jam density and discharge rate: An experimental study on a single path, *Transportation Research Part C: Emerging Technologies*, **122**, 102884, 1 2021, ISSN 0968090X.

Wierbos, M. J., V. L. Knoop, F. S. Hänseler and S. P. Hoogendoorn (2019) Capacity, Capacity Drop, and Relation of Capacity to the Path Width in Bicycle Traffic, *Transportation Research Record: Journal of the Transportation Research Board*, **2673** (5) 693–702, 5 2019, ISSN 0361-1981.

Yuan, Y., B. Goñi-Ros, M. Poppe, W. Daamen and S. P. Hoogendoorn (2019) Analysis of Bicycle Headway Distribution, Saturation Flow and Capacity at a Signalized Intersection using Empirical Trajectory Data, *Transportation Research Record: Journal of the Transportation Research Board*, **2673** (6) 10–21, 6 2019, ISSN 0361-1981.

Yuan, Y., K. Wang, D. Duives, W. Daamen and S. P. Hoogendoorn (2025) Machine learning-based bicycle delay estimation at signalized intersections using sparse GPS data and traffic control signals - A Dutch case study using random forest algorithm, *Artificial Intelligence for Transportation*, **3-4**, 100037, 11 2025, ISSN 30508606.

Zhao, Y. and H. Zhang (2017) A unified follow-the-leader model for vehicle, bicycle and pedestrian traffic, *Transportation Research Part B: Methodological*, **105**, 315–327, 11 2017, ISSN 01912615.

Zimmermann, M., T. Mai and E. Frejinger (2017) Bike route choice modeling using GPS data without choice sets of paths, *Transportation Research Part C: Emerging Technologies*, **75**, 183–196, 2 2017, ISSN 0968090X.